Available online at www.sciencedirect.com
SCIENCE DIRECT
Biochemical Pharmacology 70 (2005) 740–751
Biochemical Pharmacology
www.elsevier.com/locate/biochempharm

Protective effects of Ca^{2+} handling drugs against abnormal Ca^{2+} homeostasis and cell damage in myopathic skeletal muscle cells

Yuko Iwata [a,*], Yuki Katanosaka [a,1], Zhu Shijun [a], Yuko Kobayashi [a], Hironori Hanada [a], Munekazu Shigekawa [b], Shigeo Wakabayashi [a]

[a] *Department of Molecular Physiology, National Cardiovascular Center Research Institute, Fujishiro-dai 5-7-1, Suita, Osaka 565, Japan*
[b] *Department of Human Life Sciences, Senri Kinran University, Suita, Osaka 565-0873, Japan*

Received 3 March 2005; accepted 16 May 2005

Abstract

Deficiency of δ-sarcoglycan (δ-SG), a component of the dystrophin–glycoprotein complex (DGC), causes skeletal muscular dystrophy and cardiomyopathy in BIO14.6 hamsters. Here, we studied the involvement of abnormal Ca^{2+} homeostasis in muscle degeneration and the protective effect of drugs against Ca^{2+} handling proteins in vivo as well as in vitro. First, we characterized the properties of cultured myotubes from muscles of normal and BIO14.6 hamsters (30–60 days old). While there were no apparent differences in the levels of expression of various Ca^{2+} handling proteins (L-type Ca^{2+} channel, ryanodine receptor, SR-Ca^{2+} ATPase, and Na^+/Ca^{2+} exchanger), muscle-specific proteins (contractile actin and acetylcholine receptor), or DGC member proteins except SGs, BIO14.6 myotubes showed a high degree of susceptibility to mechanical stressors, such as cyclic stretching and hypo-osmotic stress as compared to normal myotubes, as evidenced by marked increases in creatine phosphokinase (CK) release and bleb formation. BIO14.6 myotubes showed abnormal Ca^{2+} homeostasis characterized by elevated cytosolic Ca^{2+} concentration, frequent Ca^{2+} oscillation, and increased $^{45}Ca^{2+}$ uptake. These abnormal Ca^{2+} events and CK release were significantly prevented by Ca^{2+} handling drugs, tranilast, diltiazem, and FK506. The calpain inhibitor E64 prevented CK release, but not $^{45}Ca^{2+}$ uptake. Some of these drugs (tranilast, diltiazem, and FK506) also exerted a significant protective effect for muscle degeneration in BIO14.6 hamsters and *mdx* mice in vivo. These observations suggest that elevated Ca^{2+} entry through sarcolemmal Ca^{2+} channels predominantly contributes to muscle degeneration and that the drugs tested here may have novel therapeutic potential against muscular dystrophy.

Keywords: Muscular dystrophy; Mechanical stretch; Ca^{2+} homeostasis; Ca^{2+}-permeable channel; Ca^{2+} influx; Cell damage

1. Introduction

Muscular dystrophy is a heterogeneous genetic disease that affects striated muscle (skeletal as well as cardiac muscle). The genetic defects associated with muscular dystrophy often include mutations in one of the components of the dystrophin–glycoprotein complex (DGC), such as dystrophin or sarcoglycans (α-, β-, γ-, and δ-SGs). The DGC is a multi-subunit complex [1–3] that spans the sarcolemma to form a structural link between the extracellular matrix and the actin cytoskeleton [4]. Disruption of DGC could, therefore, affect the membrane integrity or stability during muscle contraction and relaxation.

SGs are expressed predominantly in striated muscle. A genetic defect in any one of the four SGs reported to date causes an autosomal-inherited muscular dystrophy in humans [5,6]. In addition, the BIO14.6 strain of the Syrian hamster, which spontaneously develops muscular dystrophy and cardiomyopathy [7], has been shown previously to have a defect in the gene encoding δ-SG [8]. In muscles of these patients or animal models, in addition to lack of each

* Corresponding author. Tel.: +81 6 6833 5012; fax: +81 6 6835 5314.
E-mail address: yukoiwat@ri.ncvc.go.jp (Y. Iwata).
[1] Research Fellow of the Japan Society for the Promotion of Science.

0006-2952/$ – see front matter © 2005 Elsevier Inc. All rights reserved.
doi:10.1016/j.bcp.2005.05.034

primary-defective SG gene product, other components of the SG subcomplex are markedly reduced or absent, although dystrophin and β-DG are often present at mildly reduced levels [8–11]. Although little is known about the normal and pathological functions of SGs, these findings indicate that, similar to dystrophin, SGs are required for myocyte survival.

The mechanism by which the defect of DGC causes myocyte degeneration remains elusive. Myocyte degeneration has long been attributed to membrane defects, such as greater fragility towards mechanical stress or increased permeability to Ca^{2+}. A number of studies have reported chronic elevation in the cytosolic Ca^{2+} concentration ($[Ca^{2+}]_i$), beneath the sarcolemma, or within other cell compartments in skeletal muscle fibers or in cultured myotubes from dystrophin-deficient Duchenne muscular dystrophy (DMD) patients and *mdx* mice [12–14]. The $[Ca^{2+}]_i$ in muscles is regulated by multiple Ca^{2+}-permeable channels, Ca^{2+} pumps, and transporters in the plasma membrane and the sarcoplasmic reticulum (SR). Among them, a great deal of attention has focused on sarcolemmal Ca^{2+}-permeable channels (Ca^{2+}-specific leak channels) or mechanosensitive non-selective cation channels, which contribute to abnormal Ca^{2+} handling in dystrophic myocytes [15,16]. We have previously shown that δ-SG-deficient myotubes produced by treatment with antisense oligonucleotide are highly susceptible to the mechanical stretch and show the enhanced Ca^{2+} influx [17]. Subsequently, we have shown that stretch-activated non-selective Ca^{2+} channel activity was enhanced in the skeletal muscles of BIO14.6 hamsters [18]. Recently, we identified one such channel, the growth factor responsive channel (GRC), which may be involved in the pathogenesis of myocyte degeneration caused by DGC disruption [19]. While further studies are required to elucidate the pathological significance of individual Ca^{2+} channels, it is also important to address how the increased Ca^{2+} entry affects cell damage and whether pharmacological agents against Ca^{2+} handling proteins ameliorate muscle degeneration in myopathic patients or animal models.

In the present study, we performed the biochemical characterization of myotubes produced from satellite cells of control and BIO14.6 hamster skeletal muscles which were not previously reported in details, and examined the effects of several pharmacological agents, such as Ca^{2+} channel inhibitors and a Ca^{2+}-dependent phosphatase (calcineurin) inhibitor, on Ca^{2+} homeostasis and responsiveness to cyclic stretch in myotubes. Furthermore, we examined the protective effects of various drugs on muscle degeneration in vivo. The results reinforced our previous findings that mechanical weakness arose at least partly from increased Ca^{2+} influx in the dystrophic myotubes, and suggested that some drugs exerted a significant protective effect against muscle injury. To our knowledge, this is the first to show that Ca^{2+} channel inhibitor tranilast and calcineurin inhibitor FK506 are protective against muscular dystrophy.

2. Materials and methods

2.1. Animal experiments

Male BIO14.6 hamsters (J2N-k strain) between 30 and 40 days of age and age-matched normal controls (J2N-n) were used. Hamsters were anesthetized according to the Guidelines for Animal Experimentation at the National Cardiovascular Center. For examination of drug effects, diltiazem, tranilast, and FK506 were administered orally in either the drinking water or feed (for tranilast) at drug/body weight ratios of 72, 400, and 0.5 mg/kg per day, respectively, to 30-day-old BIO14.6 hamsters or *mdx* mice. After continuous administration for 30–90 days, animals were subjected to measurement of blood creatine phosphokinase (CK) level and immunohistochemistry. Immunohistochemistry of skeletal muscles was performed as described previously [10]. The numbers of total and central nuclei were counted by observing specimens on a light microscope (40× objective).

2.2. Materials

Rabbit polyclonal antibodies against rabbit α-SG and β-DG and δ-SG were described previously [20,21]. Monoclonal antibodies against dystrophin and α-actin were purchased from Novocastra (Newcastle, UK) and Biomarker (Israel), respectively. The mouse monoclonal antibody against syntrophin was described previously [22]. Antibodies against Na^+/K^+ ATPase, Na^+/Ca^{2+} exchanger 1, L-type Ca^{2+} channel, SR-Ca^{2+} ATPase, ryanodine receptor, β-SG, and γ-SG were described previously [21,23]. Antibodies against caveolin-3 and Ach receptor β were obtained from Transduction Laboratories (Franklin Lakes, NJ). Nifedipine, gadolinium chloride hexahydrate, diltiazem, and E64 were purchased from Sigma Chemical (St. Louis, MO). Tranilast was obtained from Kissei Pharmaceutical (Matsumoto city, Nagano, Japan). α-Bungarotoxin and thapsigargin were from Calbiochem (La Jolla, CA) and ruthenium red was from Wako Chemicals (Osaka, Japan). $^{45}CaCl_2$ and [^{125}I]α-bungarotoxin were purchased from NEN Life Science Products (Boston, MA). Fura-2-acetoxymethylester (AM) and fluo-4-acetoxymethylester were from Dojindo Laboratories (Tokyo, Japan) and Molecular Probes (Eugene, OR).

2.3. Cell culture

Satellite cells were isolated from the gastrocnemius muscles of 30–40-day-old hamsters by enzymatic dissociation by a slight modification of the method described by Rando and Blau [24]. Minced muscles (0.3 g) were incubated in 1 ml of Ham's F12 medium containing 2 U/ml dispase and 1% collagenase. After incubation for 45 min at 37 °C, the muscle slurry was diluted with 10 ml Ham's F12 medium (GIBCO BRL Gaithersburg, MA) and spun at

350 × *g* to sediment the dissociated cells. The cells were then resuspended in growth medium, filtered through a fine mesh nylon filter (100 μm), and subjected to preplating for 1 h at 37 °C to remove fibroblasts (differential adhesion). Non-adhering cells were plated onto collagen-coated (100 mg/ml collagen type I; Sigma) culture dishes at a density of 5000 cells/cm^2. Growth medium for myoblasts consisted of Ham's F12 medium supplemented with 20% FCS and 2.5 ng/ml bFGF (Promega BRL Madison, WI) and 1% chick embryo extract (GIBCO BRL). When myoblasts had reached 80% confluence, they were trypsinized and then plated on collagen-coated dishes for experiments. During the first several passages of the primary cultures, myoblasts were enriched by preplating. After 1–2 days, medium was changed to DMEM (GIBCO BRL) containing 2% horse serum (Hyclone Laboratories, Logan, UT) to initiate differentiation. Myoblasts begin to fuse and form myotubes in culture within 24 h. We used the myotubes 2–5 days after the first myotubes had formed.

2.4. Measurement of $^{45}Ca^{2+}$ uptake and cellular content of exchangeable Ca^{2+}

Myotubes from normal and BIO14.6 skeletal muscles were cultured on collagen I-coated silicon membranes or in 24-well dishes and preincubated at 37 °C for 30 min in BSS (146 mM NaCl, 4 mM KCl, 2 mM $MgCl_2$, 1 mM $CaCl_2$, 10 mM glucose, 0.1% bovine serum albumin and 10 mM HEPES/Tris, pH 7.4) containing 0 or 0.5 mM $GdCl_3$. $^{45}Ca^{2+}$ uptake into cells was initiated by switching to BSS containing $^{45}CaCl_2$ (10 μCi/ml). After appropriate intervals, cells were washed four times with ice-cold 5 mM $LaCl_3$ and 10 mM HEPES/Tris, pH 7.4, to terminate $^{45}Ca^{2+}$ uptake. Cells were lysed in 0.1N NaOH and aliquots were taken for determination of protein and radioactivity. The Gd^{3+}-inhibitable fraction of $^{45}Ca^{2+}$ uptake was calculated by subtracting the uptake in the absence of Gd^{3+} from that in its presence, which accounted for about 20% of total uptake. For measurement of exchangeable Ca^{2+}, myotubes were loaded with $^{45}CaCl_2$ for 4 h at 37 °C. The cellular $^{45}Ca^{2+}$ content was measured after rinsing the myotubes five times with 1 ml of ice-cold La^{3+} solution containing 146 mM choline chloride, 4 mM KCl, 2 mM $MgCl_2$, 10 mM glucose, 10 mM HEPES/Tris (pH 7.4), and 1 mM $LaCl_3$. Cells were then solubilized with 1 ml of 0.1 M NaOH, and aliquots were taken for determination of protein and radioactivity.

2.5. Intracellular Ca^{2+} measurement

For Ca^{2+} imaging, cells were plated on glass cover slips and loaded with 4 μM fluo-4-acetoxymethyl ester (Molecular Probes) in BSS by incubation for 30 min at 37 °C. Fluorescence signals in the cells were detected by confocal laser scanning microscopy using a Bio-Rad MRC-1024ES system (Bio-Rad, Richmond, CA) mounted on an Olympus BX50WI microscope with a ×60-water immersion lens. An argon laser was used to excite fluo-4 at 488 nm. Images were acquired at a rate of one image every second and analysis of single-frame or single cell-integrated signal density was performed with LaserSharp software (Bio-Rad). The Ca^{2+} level was represented as $\Delta F/F_o$, where F_o is the resting fluo-4 fluorescence and ΔF is the difference between the basal and peak steady-state fluorescence within 1–2 min after stimulation (addition of extracellular Ca^{2+}). In some experiments, cells were loaded with 4 μM fura-2 acetoxymethyl ester with other conditions as described above and $[Ca^{2+}]_i$ was measured by a ratiometric fluorescence method using a fluorescence image processor (Argus 50, Hamamatsu Photonics, Hamamatsu, Japan) mounted on a Nikon inverted microscope (×40 objective). The excitation wavelength was alternated at 340 and 380 nm (1 Hz), while the fluorescence was monitored at 510 nm. $[Ca^{2+}]_i$ was calculated from the fluorescence ratio $R_{340/380}$ using a K_d of 224 nM for the dissociation constant of fura-2/Ca^{2+} [25].

2.6. Application of cell stretch to myotubes

Mechanical stretching was applied to myotubes using a chamber similar to that used by Naruse and Sokabe [26]. The silicon chamber with a transparent bottom 200 μm thick was attached to a stretching apparatus that was driven by a computer-controlled stepping motor. Cells were allowed to attach to the chamber bottom for the indicated times, and mono-axial sinusoidal stretching was applied to the silicon chamber at a constant strength from 5 to 20% elongation at 1 Hz. The relative elongation of the silicone membrane was uniform across the whole membrane area. Stretching experiments were performed at 25 ± 1 °C. Osmotic stress-induced cell damage was observed in myotubes preloaded with 5 μM calcein-AM (Molecular Probes).

2.7. Enzyme assay and other procedures

Creatine phosphokinase activity in medium was determined using an in vitro colorimetric assay kit (CK Test Kit, Wako Pure Chem. Co., Osaka, Japan) according to the protocol provided by the manufacturer. CK contents in myotubes were also measured using the above method after homogenization. For [^{125}I]α-bungarotoxin binding assay, myoblasts and myotubes were incubated for 1 h at 37 °C in DMEM containing 20 nM [^{125}I]α-bungarotoxin. Non-specific binding of radiolabeled toxin was measured in the presence of 2 μM non-radiolabeled α-bungarotoxin or 10 μM acetylcholine chloride. Cells were solubilized with 0.1N NaOH and aliquots were taken for determination of protein and radioactivity. Quantitative immunoblotting analysis and immunocytochemistry were performed as described previously [20,21,23]. Protein concentration was measured using a bicinchoninic acid

assay system (Pierce Chemical Co., Rockford, IL) with bovine serum albumin as a standard. Unless otherwise stated, data were represented as means ± S.D. of at least three determinations. We used an unpaired *t*-test, one-way ANOVA followed by Dunnett's test or two-way ANOVA for statistical analyses. Values of $p < 0.05$ were considered statistically significant.

3. Results

3.1. Characterization of myotubes from normal and BIO14.6 hamsters

We isolated satellite cells from skeletal muscles of normal and BIO14.6 hamsters (see Section 2). Satellite cells from both normal and BIO14.6 hamsters grew at similar rates in the growth medium containing 20% FCS and 10 ng/ml bFGF. The bFGF was required for the optimal growth of cells from both hamster strains. Two days after cell plating, we stained for the muscle-specific protein desmin to evaluate the purity of cultures. Desmin is an intermediate filament present only in myogenic cells but not in non-myogenic cells, such as fibroblasts. Desmin-positive cells accounted for 96 and 97% of cultures from normal and myopathic hamsters, respectively. Then, we switched the growth medium to the differentiation medium containing 2% horse serum. Satellite cells began to fuse rapidly after switching to the differentiation medium and formed well-differentiated myotubes. Staining of actin with rhodamine-conjugated phalloidin indicated that myotubes from both muscles have similar sarcomeric patterns (Fig. 1A). These myotubes were stained with antibodies against muscle marker proteins. As expected, myotubes

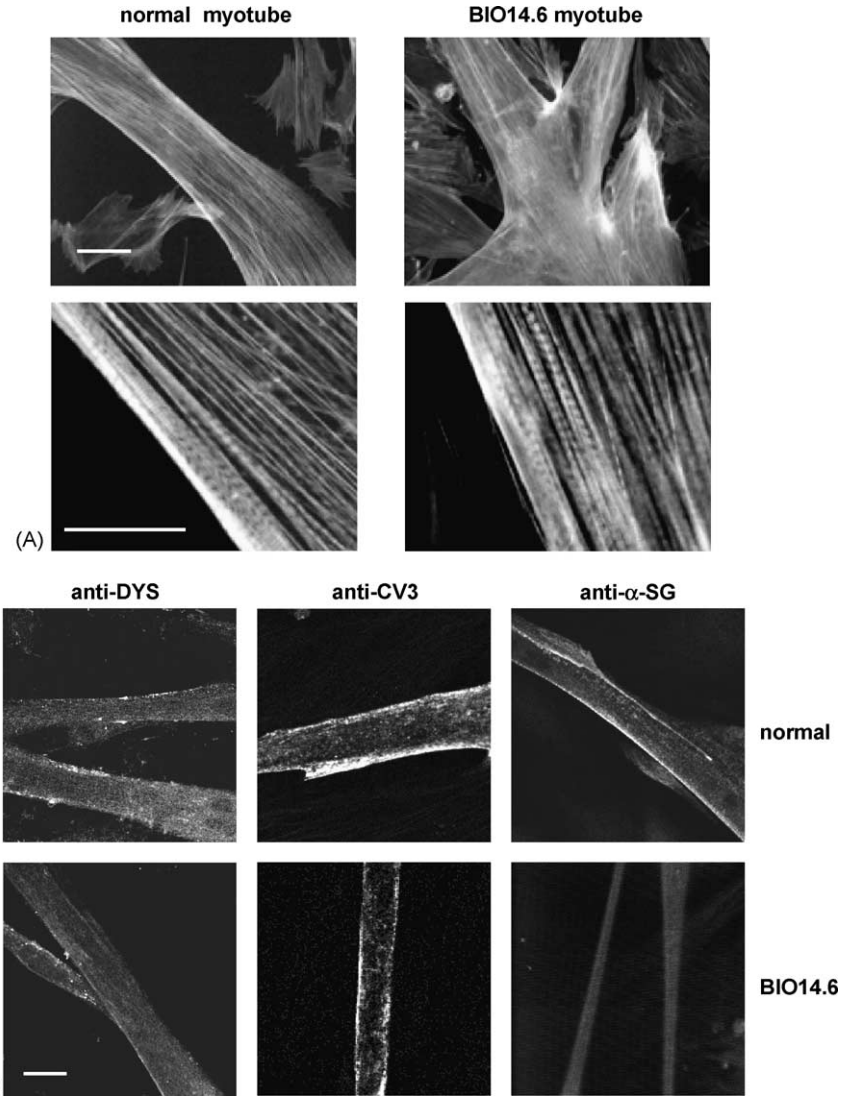

Fig. 1. Morphology of myotubes from normal and BIO14.6 hamster skeletal muscles. (A) Actin staining pattern. Myotubes from normal (left) and BIO14.6 (right) hamster skeletal muscles were formed by exposure to the differentiation medium for 2 days and stained with rhodamine–phalloidin. The scale bars indicate 50 (upper panel) or 10 μm (lower panel). (B) Dystrophin (DYS), caveolin-3 (CV3), and α-sarcoglycan (α-SG) localization were examined by staining with the respective antibodies in control and BIO14.6 myotubes. The scale bar indicates 50 μm.

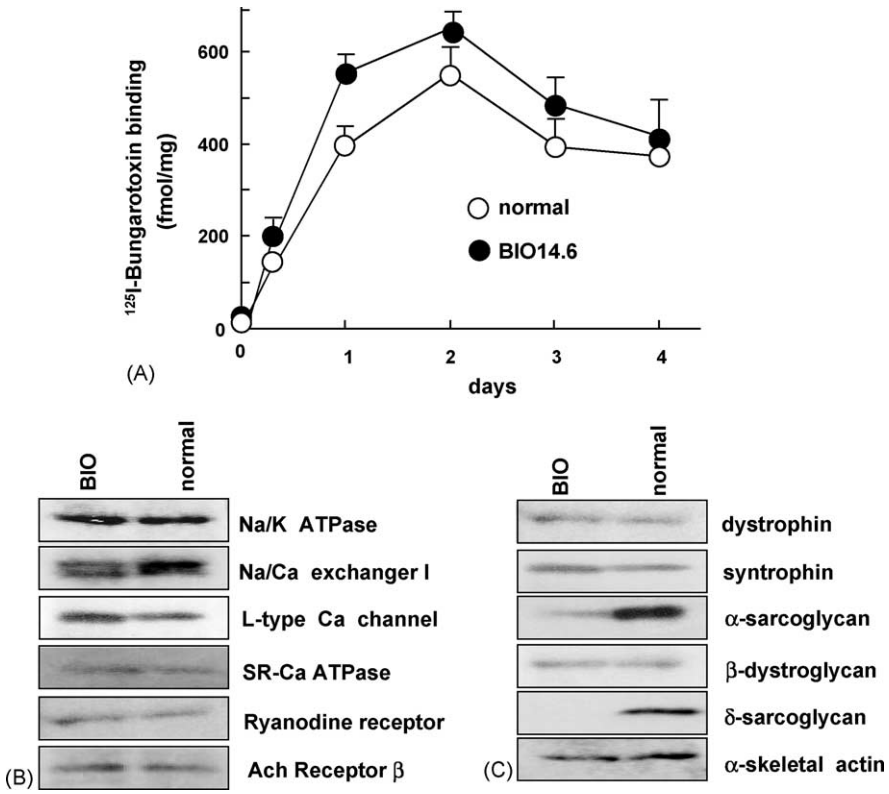

Fig. 2. Biochemical characterization of myotubes. (A) ^{125}I-bungarotoxin binding to myotubes. After plating, cells were exposed to the differentiation medium on day 0, and ^{125}I-bungarotoxin binding was measured as described in Section 2. Data are means ± S.D. of three determinations. (B and C) Comparison of expression levels of several membrane (B) and cytoskeletal proteins (C) between normal and BIO14.6 myotubes. Myotubes were formed during 2–3 days in differentiation medium and homogenates (40 μg each) were subjected to SDS-polyacrylamide gel electrophoresis followed by immunoblotting analysis using the respective antibodies. These immunoblot analyses were repeated more than three times and essentially the same results were obtained.

from BIO14.6 hamsters were not stained with anti-α-SG, while the peripheral membrane regions in myotubes from normal hamsters showed clear staining (Fig. 1B, right panels). In contrast, peripheral regions were stained with anti-caveolin-3, anti-dystrophin (Fig. 1B), and anti-β-DG (data not shown) in myotubes from both normal and BIO14.6 hamsters.

We next examined differentiation-dependent changes in myotube-specific markers. As shown in Fig. 2A, when cells were exposed to the differentiation medium, the amount of ^{125}I-bungarotoxin binding rapidly increased, reached a maximum at day 2, and then decreased slightly in cultures from both normal and BIO14.6 hamsters, suggesting that the acetylcholine receptors developed similarly in both cases during myotube formation. The same level of expression of Ach receptor in both cultures was also confirmed by immunoblotting analysis (see Fig. 2B). Consistent with this finding, cellular content of another muscle-specific enzyme, creatine phosphokinase, also increased during myotube formation similarly in both cultures (data not shown). Immunoblotting analysis indicated that myotubes from normal and BIO14.6 hamster muscles expressed similar levels of cellular Ca^{2+} regulatory proteins, such as L-type Ca channels ryanodine receptors, SR-Ca^{2+} ATPase and Na^+/Ca^{2+} exchanger in cultures from normal and BIO14.6 hamsters (Fig. 2B). Relative amount of these proteins in BIO14.6 to normal myotubes estimated from the density of protein bands were 1.10 ± 0.20, 1.00 ± 0.05, 1.08 ± 0.05 and 0.95 ± 0.03 (means ± S.D. of three determinations), respectively. While similar amounts of dystrophin, dystrophin-associated proteins (syntrophin and β-DG), and actin were detected, the amounts of α-, β- and γ-SGs were significantly reduced (Fig. 2C; data not shown for β- and γ-SGs). δ-SG was completely absent from BIO14.6 myotubes (Fig. 2C). These results suggest that primary cultures of myotubes from normal and BIO14.6 hamsters possess muscle-type morphological and biochemical properties that are close to those of skeletal muscles in vivo. For most experiments, we used myotubes 2–3 days after switching to the differentiation medium because the maximal levels of expression of muscle-specific proteins were detected at this stage. Myotubes cultured for more than 3 days became very thin and were prone to be detached from the dishes.

3.2. Abnormal Ca^{2+} handling in BIO14.6 myotubes and effect of various pharmacological agents

To measure the cellular ^{45}Ca content, cells were loaded with $^{45}CaCl_2$ for 4 h (see Section 2). We found that it was not significantly different between normal (2.95 ± 0.35

nmol/mg, $n = 3$) and BIO14.6 myotubes (3.01 ± 0.32 nmol/mg, $n = 3$). In addition, we observed that the Ca^{2+} ionophore ionomycin was able to raise the intracellular Ca^{2+} concentration to similar maximal levels for normal and BIO14.6 myotubes. Thus, the amount of cellular exchangeable Ca^{2+} appeared to be almost the same between the two kinds of myotubes. This may reflect the same capacity of Ca^{2+} storage, as suggested by the same level of SR-Ca^{2+} ATPase (see Fig. 2B).

In contrast, we found that the resting state of mean $[Ca^{2+}]_i$ appeared to be significantly higher ($p < 0.05$) in BIO14.6 myotubes (122 ± 13 nM, $n = 6$) than in those from normal controls (86 ± 18 nM, $n = 6$) when $[Ca^{2+}]_i$ was measured by ratiometric fluorometry with fura-2. Furthermore, we observed very often irregular cytosolic Ca^{2+} oscillation via cytosolic Ca^{2+} overload in dystrophic myotubes when fluo-4-loaded cells were placed even at relatively low extracellular Ca^{2+} concentration (Fig. 3A upper) (43 myotubes oscillated/100 myotubes). Further addition of 2 mM Ca^{2+} in the extracellular medium markedly raised $[Ca^{2+}]_i$ and evoked more extensive Ca^{2+} oscillation in BIO14.6 myotubes, while the same treatment did not induce marked increases in $[Ca^{2+}]_i$ in normal controls (Fig. 3A lower). Next, we examined the effects of several pharmacological agents on the increase in $[Ca^{2+}]_i$. The extracellular Ca^{2+}-induced increase in $[Ca^{2+}]_i$ and Ca^{2+} oscillation were significantly inhibited by the Ca^{2+} channel antagonist diltiazem (Fig. 3B), but not by nifedipine. It was also of interest for us to study whether an antiallergic drug tranilast and Ca^{2+}-dependent phosphatase (calcineurin) inhibitor FK506 inhibit the increase in $[Ca^{2+}]_i$ because the former was reported to inhibit IGF1-induced cell growth through inhibition of Ca^{2+} entry [27] and the latter modulates the Ca^{2+} homeostasis through calcineurin inhibition. As shown in Fig. 3B, both tranilast and FK506 effectively inhibited Ca^{2+}-induced increase in $[Ca^{2+}]_i$ (Fig. 3C).

To determine whether the increase in $[Ca^{2+}]_i$ was due to either enhancement of Ca^{2+} entry or reduction of the Ca^{2+} extrusion pathways, we measured the $^{45}Ca^{2+}$ uptake activity. We also measured $^{45}Ca^{2+}$ uptake in the presence of a high concentration (500 μM) of $GdCl_3$ to subtract the non-specific binding of $^{45}Ca^{2+}$ to the cell surface and represented the data as the Gd^{3+}-inhibitable fraction of ^{45}Ca uptake. The $^{45}Ca^{2+}$ uptake activity was significantly greater in BIO14.6 myotubes than in those from normal controls, reaching a level 1.7-fold higher at 5 min (Fig. 4A). Consistent with the effect on $[Ca^{2+}]_i$ (see Fig. 3C), diltiazem, tranilast, and FK506 markedly inhibited $^{45}Ca^{2+}$ uptake activity, while E64 and nifedipine had no effect (Fig. 4B).

3.3. Effects of various pharmacological agents on muscle degeneration in vitro and in vivo

To examine the effects of mechanical stress on myotube degeneration, we applied cyclic stretching up to 20% elongation for 1 h to normal and BIO14.6 myotubes and

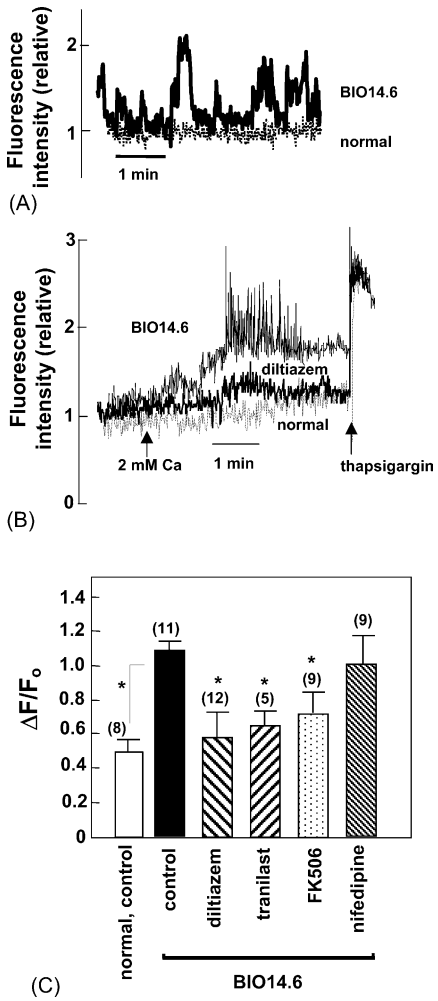

Fig. 3. Abnormal Ca^{2+} homeostasis in BIO14.6 hamster myotubes. (A upper and lower) Typical traces for changes in the fluo-4 fluorescence intensity in normal and BIO14.6 myotubes. In the presence of 0.5 mM extracellular Ca^{2+}, irregular cytosolic Ca^{2+} oscillation was observed in only BIO skeletal myotubes, but not in normal myotubes (A upper). Addition of 2 mM $CaCl_2$ (final, 2.5 mM) induced a rapid increase in $[Ca^{2+}]_i$ with high frequency Ca^{2+} oscillation in BIO14.6 myotubes (A lower). In one experiment, diltiazem (10 μM) was added to the medium at 30 min before Ca^{2+} addition. Thapsigargin (1 μM) was used to estimate the Ca response. (B) The effects of various pharmacological agents on the relative fluorescence intensity. Myotubes were exposed for 30 min to 10 μM diltiazem, 100–500 μM tranilast, 2 μM FK506 or 0.1 μM nifedipine before addition of 2 mM $CaCl_2$. The extracellular Ca^{2+}-dependent increment (ΔF, 2 min after Ca^{2+} addition) in the fluorescence intensity was calculated and represented as $\Delta F/F_o$ after normalization with the initial fluorsecence (F_o). Data are means ± S.D. (trial numbers are shown in parentheses). $^{*}p < 0.05$ (vs. control for drug effect).

monitored the activity of CK released into the medium from these cells. As previously reported by us [17,19], CK release increased in an elongation-dependent manner and reached more than 10-fold after stretching of BIO14.6 myotubes, while it did not change in normal myotubes (Fig. 5A). Consistent with stretch-induced cell injury in BIO14.6 myotubes, the stretch (>5%) resulted in dystrophin degradation accounting for more than 70% of dystrophin in the membranes, which was prevented by the calpain inhibitor E64 (data not shown). In addition,

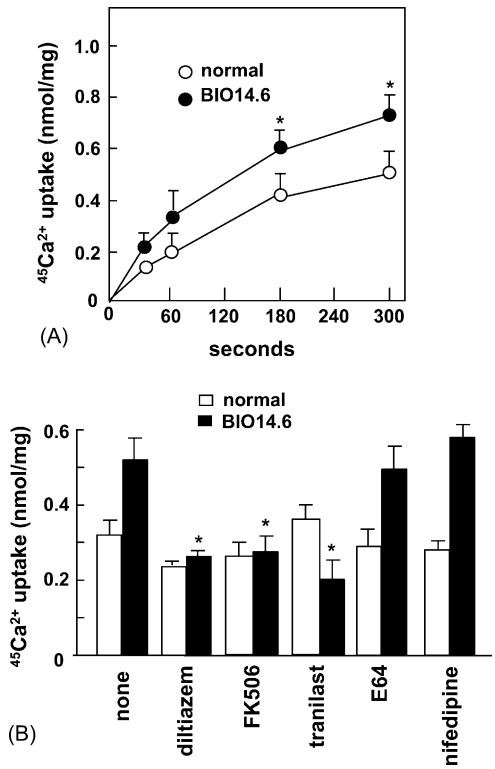

Fig. 4. Effects of various pharmacological agents on $^{45}Ca^{2+}$ uptake activity. (A) Time courses of $^{45}Ca^{2+}$ uptake into control and BIO14.6 myotubes. $^{45}Ca^{2+}$ uptake was started by replacing the BSS medium with BSS containing 1 mM $^{45}Ca^{2+}$ and stopped at appropriate times. Ca^{2+} uptake was also measured in the presence of 500 μM $GdCl_3$ to estimate non-specific $^{45}Ca^{2+}$ binding to the cell surface. Data are represented as Gd^{3+}-inhibitable fractions of $^{45}Ca^{2+}$ uptake that accounted for about 80% of the total $^{45}Ca^{2+}$ uptake (means ± S.D. of three determinations). $^{*}p < 0.05$. (B) Myotubes were exposed for 30 min to 10 μM diltiazem, 2 μM FK506, 100–500 μM tranilast, 1 mM E64 or 0.1 μM nifedipine and then Gd^{3+}-sensitive $^{45}Ca^{2+}$ uptake was measured over a period of 5 min. Data are means ± S.D. of three determinations. $^{*}p < 0.05$ (vs. no drug control for BIO14.6 myotubes).

TUNEL- and annexin V-positive cells (1–3%) were detected under 20% elongation in cultures from BIO14.6 but not from normal hamsters, suggesting that a proportion of BIO14.6 myotubes enter the apoptotic cell death pathway. Mechanical weakness of BIO14.6 myotubes was also observed under hypo-osmotic stress (70% osmolarity). Upon hypo-osmotic stimulation, extensive formation of cell blebs was observed in BIO14.6, but not in normal myotubes (15 ± 5 blebs/BIO myotube; 4 ± 3 blebs/normal myotube, $n = 10$) (Fig. 6). All these data suggest that myotubes from BIO14.6 are highly susceptible to the mechanical stretch.

We examined the effects of pharmacological agents on CK release in BIO14.6 myotubes. Myotubes were treated with each agent for 30 min and then subjected to cyclic stretching (20% elongation) for 1 h. All of the agents tested showed significantly inhibited CK release from BIO14.6 myotubes. Diltiazem (10 μM), E64 (1 mM), FK506 (1 μM) and tranilast (100–500 μM) reduced stretch-induced CK release from myotubes by up to 70%

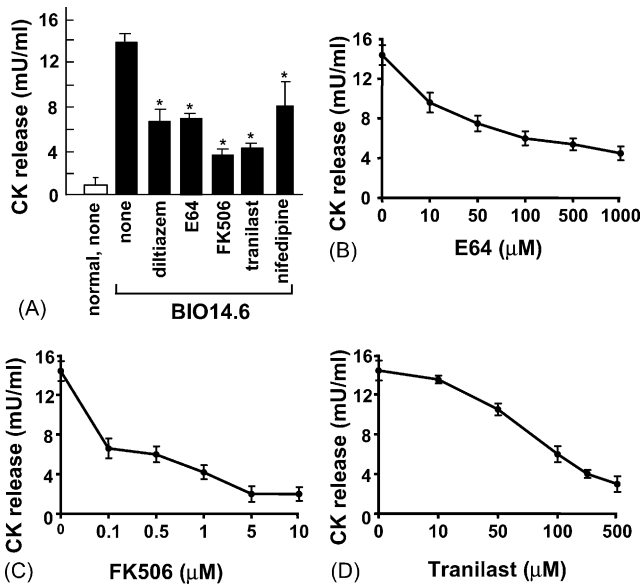

Fig. 5. Effects of various pharmacological agents on stretch-induced CK release from BIO14.6 myotubes. (A) Myotubes from normal or BIO14.6 hamsters were preincubated in the absence or presence of 10 μM diltiazem, 2 μM FK506, 100–500 μM tranilast, 1 mM E64, or 0.1 μM nifedipine subjected to cyclic stretching (20%) for 1 h, and the activity of CK released into the medium was measured. Data are means ± S.D. of three determinations. $^{*}p < 0.05$. (B–D) BIO14.6 myotubes were subjected to stretching after exposure to the indicated concentrations of E64, FK506, or tranilast, and the CK activity was measured. Data are means ± S.D. of three determinations.

(Fig. 5A). The inhibitory effects of E64, FK506 and tranilast were dose-dependent, with half-maximal inhibition occurring at about 50, 0.5, and 75 μM, respectively (Fig. 5B–D). Cyclosporin A (CsA) also reduced the

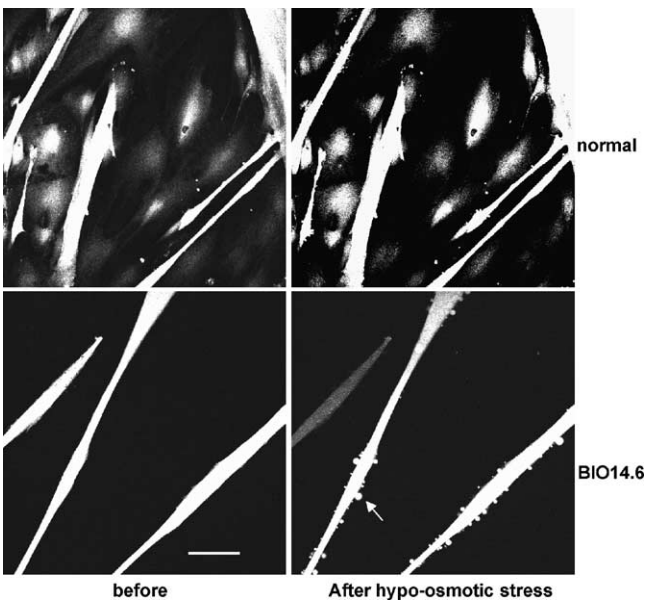

Fig. 6. Hypo-osmotic stress-induced cell damage in dystrophyc myotubes. Normal and BIO14.6 myotubes were preloaded with 5 μM calcein-AM and exposed for 17 min to hypo-osmotic medium (70% osmolarity). Extensive bleb formation was observed in BIO14.6 myotubes (arrow). The scale bar indicates 50 μm.

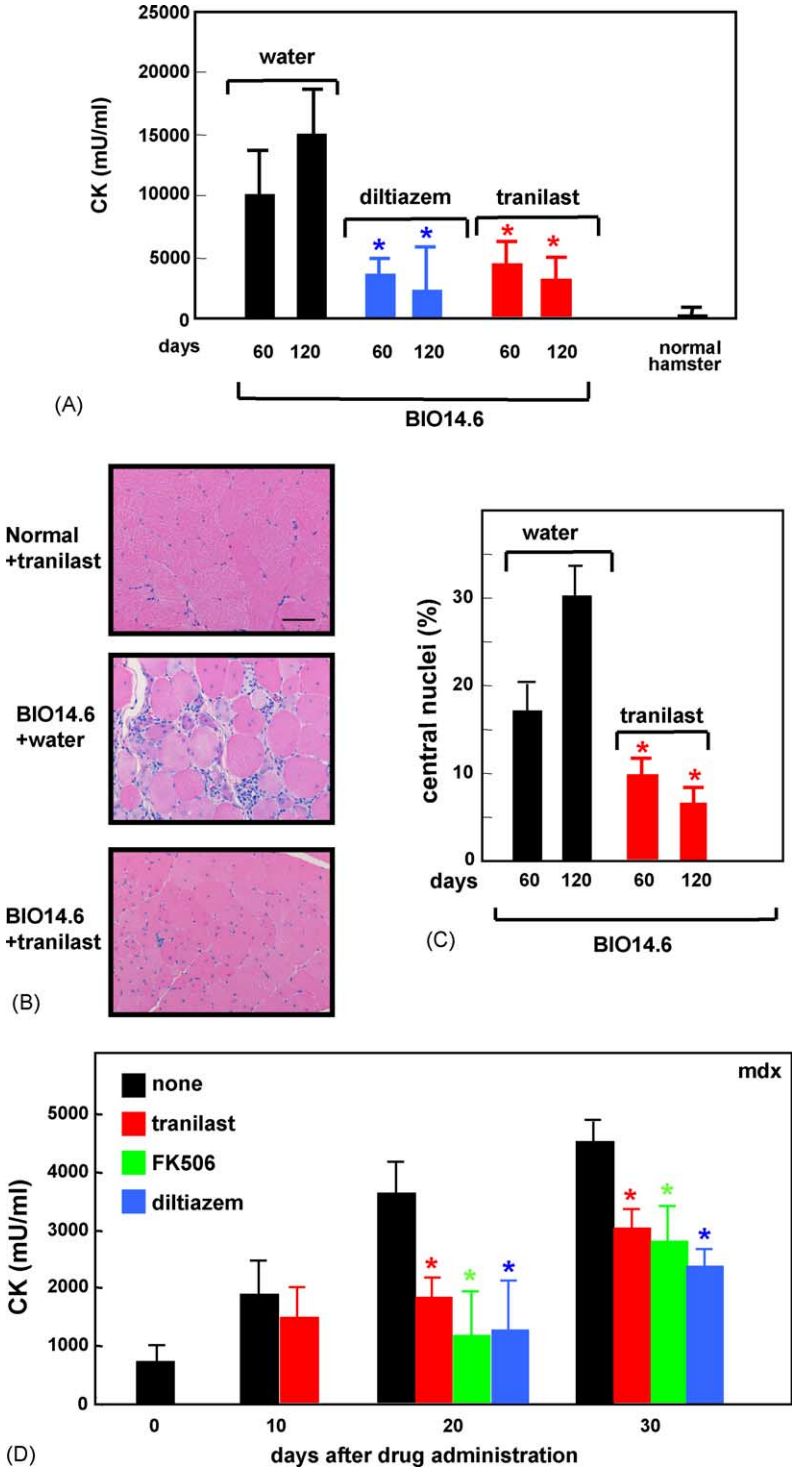

Fig. 7. Effects of various pharmacological agents on muscle degeneration in BIO14.6 hamsters and *mdx* mice. (A) CK level in blood from BIO14.6 hamsters. Diltiazem and tranilast were administered orally to 30-day-old BIO14.6 hamsters up to 120 days and blood CK level was measured. For one control, the blood CK level of 60-day-old normal hamsters is shown. Data are means ± S.D. ($n = 3$–5) $^{*}p < 0.05$. (B) Gastrocnemius muscle samples were taken from normal hamsters treated with tranilast or from BIO14.6 administrated with water or tranilast for 90 days and sections were stained with hematoxylin (red) and eosin (blue). Scale bar, 100 μm. (C) Percentage of centrally nucleated fibers. For experiment, skeletal muscles from three hamsters were used and more than 1000 fibers were examined for each experiment. $^{*}p < 0.05$ (vs. water control). (D) Effects of various drugs on blood CK level. Drug administration was started in 30-day-old *mdx* mice (day 0). Data are means ± S.D. ($n = 5$) $^{*}p < 0.05$.

stretch-induced CK release (data not shown) with half-maximal inhibition at 1 μM. As reported previously [19], Gd^{2+} (500 μM) and ruthenium red (5 μM) were much more effective (more than 90% inhibition) for inhibition of CK release, while nifedipine significantly (~40%) inhibited CK release (Fig. 5A).

Finally, we examined the effects of oral administration of pharmacological agents on myopathic animals. As

shown in Fig. 7A, diltiazem and tranilast markedly reduced the blood CK level in BIO14.6 hamsters during the period of 30–90 days after drug administration. Furthermore, tranilast (Fig. 7B) and diltiazem (not shown) greatly ameliorated muscle degeneration and fibrosis as shown in sections stained with hematoxylin and eosin. The number of central nuclei was markedly reduced under treatment with tranilast (Fig. 7C). We next used *mdx* mice, another myopathic animal model, to examine the effects of several drugs, because *mdx* mice have the advantage that blood can be obtained easily from their tails without killing the animals. As shown in Fig. 7D, similar to BIO14.6 hamsters, diltiazem was effective in reducing the blood CK level. Tranilast and FK506 were also as effective as diltiazem (Fig. 7D).

4. Discussion

4.1. BIO14.6 myotubes in culture as a useful model system to study the effects of δ-SG deficiency

In the present study, we characterized biochemical and pathological properties of culture myotubes from δ-SG-deficient BIO14.6 and normal hamsters. Both myotubes possess well-developed myofibrils and apparently normal plasma membrane structure as shown by immunostaining with anti-actin and anti-caveolin-3, of which the latter's sarcolemmal expression is known to be a good marker for well-differentiated skeletal muscle cells [28]. In addition, both types of myotubes expressed similar levels of various ion transporters and channels. After switching to the differentiation medium, myotubes from both strains expressed Ach receptor (see Fig. 2A) and CK (data not shown) with similar time courses. Among the members of the dystrophin complex, δ-SG was completely absent from BIO14.6 myotubes, while expression level and sarcolemmal localization of other α-, β- and γ-SGs were greatly reduced. These biochemical properties are similar to those observed in native muscles (our unpublished data). Thus, this in vitro system would allow us to study the effect of δ-SG deficiency on various cellular functions including ion flux and apoptosis under some stresses during relatively short period. Previously, we analyzed the effects of δ-SG deficiency on cell function using L6 myotubes transfected with antisense oligonucleotides against δ-SG [17,21]. However, it was difficult to deplete δ-SG completely by this technique. Recently, satellite cells were isolated from dystrophic hamsters by another group [29]. However, their myotubes from normal hamsters detached immediately after fusion and the level of CK expression appeared to be low [29].

4.2. Abnormal Ca^{2+} homeostasis in BIO14.6 myotubes

Myotubes from BIO14.6 hamsters show abnormal intracellular Ca^{2+} homeostasis. Addition of a high concentration of external Ca^{2+} resulted in the increase in $[Ca^{2+}]_i$ and very often induced the spontaneous Ca^{2+} oscillation (Fig. 3A). Although normal skeletal muscle cells maintain a low free calcium concentration at rest to remain excitable, an increase in the resting $[Ca^{2+}]_i$ is known to often evoke spontaneous Ca release from the SR thereby causing Ca^{2+} waves or Ca^{2+} oscillation [30]. Therefore, such Ca^{2+} oscillation in BIO14.6 myotubes is probably due to intracellular Ca^{2+} overload. Indeed, $[Ca^{2+}]_i$ appeared to be slightly higher in BIO14.6 myotubes as compared to normal controls even in the resting state, and thus it would be easier to cause intracellular sparks through Ca^{2+}-induced Ca^{2+} release.

Elevated $[Ca^{2+}]_i$ may be due to: (i) abnormal Ca^{2+} storage ability in the SR, (ii) enhanced Ca^{2+} entry across the sarcolemma, or (iii) reduced Ca^{2+} extrusion from the cells. We could not detect any differences in the expression level of SR Ca^{2+}-ATPase between normal and BIO14.6 myotubes. In addition, the amount of cellular exchangeable Ca^{2+} appeared to be almost the same between the two kinds of myotubes. Thus, the size of the Ca^{2+} store in SR appears to be normal in BIO14.6 myotubes. In contrast, we observed that the $^{45}Ca^{2+}$ uptake by BIO14.6 myotubes was significantly higher than that of normal controls. While the Ca^{2+} channel blocker diltiazem significantly reduced both the rise in $[Ca^{2+}]_i$ and enhanced $^{45}Ca^{2+}$ uptake, the more specific L-type Ca^{2+} channel blocker nifedipine did not [19]. Thus, elevated $[Ca^{2+}]_i$ appears to result from some other Ca^{2+} entry pathways, including the stretch-activated channel that we reported previously [18] and the Ca leak channel observed previously in *mdx* myotubes [15]. Recently, we identified one such Ca^{2+} channel, TRPV2 (or GRC) [19]. Using Chinese hamster ovary cells stably expressing GRC, we examined the effects of Ca^{2+} handling drugs on extracellular Ca^{2+}-induced increase in $[Ca^{2+}]_i$. While tranilast effectively blocked the rise in $[Ca^{2+}]_i$ (~75% inhibition at 300 μM), 100 μM diltiazem and 1 μM FK506 moderately reduced it (20–30% inhibition) (unpublished observations). In contrast, nifedipine had no detectable effect on it. Thus, the effect of tranilast may be exerted mainly through inhibition of GRC. However, the inhibitory effects of diltiazem and FK506 may be only partly exerted through GRC.

4.3. Protective effect of Ca^{2+} handling drugs

We tested various agents for their ability to inhibit stretch-induced CK release from BIO14.6 myotubes. The Ca^{2+} channel blockers diltiazem and nifedipine, and the Ca^{2+}-dependent thiol protease (calpain) inhibitor E64 were effective in reducing CK release when applied to cells 30 min before the stretch (Fig. 5A). This is consistent with our previous results obtained in L6 and skeletal myotubes treated with antisense oligonucleotide against δ-SG [17]. We previously showed that ruthenium red and Gd^{2+}, which

inhibit Ca^{2+} influx, also markedly prevented CK release [19]. These results strongly suggest that elevated $[Ca^{2+}]_i$ is a key factor responsible for muscle dysgenesis. An increase in $[Ca^{2+}]_i$ would activate the Ca^{2+}-dependent protease calpain, which degrades dystrophin and other cytoskeletal proteins, such as fodrin. In fact, we observed that cyclic stretching resulted in proteolysis of dystrophin in BIO14.6 myotubes (see Section 3). Thus, the activation of proteolysis caused by increased $[Ca^{2+}]_i$ seems to be responsible for the observed loss of mechanical stability of myotubes. The importance of $[Ca^{2+}]_i$ would also be true for other types of dystrophy. In the muscle from *mdx* mice or DMD patients, the sarcolemma is mechanically weakened as evidenced by the observation that dystrophin-deficient myotubes or fibers are easily damaged by hypo-osmotic stress and are unable to withstand applied mechanical stress [31]. Furthermore, basal activities of Ca^{2+}-selective leak channels and/or mechanosensitive non-selective cation channels were reported to be significantly elevated in dystrophin-deficient myotubes or skeletal muscle fibers [16,32]. In these dystrophin-deficient myotubes, proteolysis was reported to be elevated especially in the presence of high extracellular Ca^{2+} [33].

In the present study, we found that tranilast was effective for inhibition of the stretch-induced CK release in BIO14.6 myotubes (Fig. 5) and for muscle degeneration and fibrosis in BIO14.6 skeletal muscles in vivo (Fig. 7). Tranilast was developed originally for the treatment of allergy and keloid formation [34,35] and has recently been used successfully to reduce experimental intimal thickening and clinical angiographic restenosis [36] or to suppress atherosclerosis [37] inhibiting proliferation of smooth muscle cells. We do not exclude the possibility that the observed protective effect in vivo may result from cardiovascular targeted effects of tranilast. However, our present findings that tranilast directly inhibits the Ca^{2+} uptake and CK release from cultured myotubes, rather suggest that it exerts the direct effect on skeletal muscles. Indeed, tranilast has been reported to inhibit the contraction of vascular smooth muscle [38] and IGF1-induced cell growth through inhibition of Ca^{2+} entry [27]. As discussed in the previous Section 4.2, the protective effect of tranilast may result from inhibition of GRC channel, because tranilast inhibited the increase in $[Ca^{2+}]_i$ in GRC-expressing fibroblastic cells, consistent with our previous finding [19] that GRC is a key player in muscular dysgenesis. Recently, effects of stretch-activated channel blockers on *mdx* muscle damage was reported [39]. They reported that two stretch-activated channel blockers, streptomycin and spider venom toxin GsMTx4, can prevent the rise of resting $[Ca^{2+}]_i$ and may protect against muscle damage in *mdx* mouse. We also observed that these drugs prevented $[Ca^{2+}]_i$ oscillation and reduced Gd^{3+}-sensitive Ca^{2+} influx in our δ-sarcoglycan-deficient BIO myotubes (unpublished observation), however, the inhibitory effect of these dugs were weaker than that of tranilast. Thus, tranilast preventing stretch-activated channel may have potential as a novel therapeutic drug against muscular dystrophy.

We also observed that FK506 and cyclosporin A (not shown) inhibit CK release in vivo as well as in vitro (Figs. 5 and 7). FK506 and CsA are widely used as immunosuppressive agents, which mostly prevent host rejection of engrafted organs, while FK506 causes severe rhabdomyolysis [40]. FK506 and CsA inhibit calcineurin through interaction with endogenous immunophilin proteins, FK-binding protein (FKBP) and cyclophilin A, respectively [41]. Recently, FK506 was reported to alter the activities of L-type Ca channels [42] and TRPC [43] through effects on FKBP12 and FKBP12.6, while CsA was reported to influence the Ca^{2+} leak pathway through the lipid bilayer and alter L-type calcium channel activity [44]. These findings suggest that FK506 is capable of altering various cellular functions in a calcineurin-dependent or independent manner. The results of the present study indicating that FK506 reduces $[Ca^{2+}]_i$ and inhibits $^{45}Ca^{2+}$ uptake, suggest that calcineurin and/or FK-binding proteins may regulate novel target molecules. Recently, we found that FK506 restores the Na^+/Ca^{2+} exchange activity inhibited by calcineurin in hypertrophied cardiomyocytes [45]. Therefore, it is possible that FK506 contributes to the reduced $[Ca^{2+}]_i$ by enhanced Ca^{2+} extrusion through activation of Na^+/Ca^{2+} exchange.

It is noted that diltiazem and nifedipine exert the protective effect in dytrophic muscles or myotubes, suggesting that L-type Ca^{2+} channel may contribute to muscle dysgenesis. However, diltiazem inhibited more strongly the rise in $[Ca^{2+}]_i$ and $^{45}Ca^{2+}$ uptake as compared to nifedipine. We do not know about the reason for these different effects. Since diltiazem but not nifedipine, partly (20–30%) inhibited the rise in $[Ca^{2+}]_i$ in GRC-expressing cells, the protective effect of diltiazem may be exerted partly through inhibition of GRC. Diltiazem was also reported to affect on various Ca^{2+} regulatory proteins such as sarcoplasmic reticulum Ca^{2+} pump [46] and Na^+/Ca^{2+} exchange [47]. Such multiple actions of diltiazem may explain the apparently beneficial effect on muscular dystrophy and the strong inhibitory effect on the rise in $[Ca^{2+}]_i$ observed in our experiments.

In summary, using an in vitro system we reinforced our previous findings [17–19] that the loss of δ-SG enhances the susceptibility of BIO14.6 myotubes to applied mechanical stress leading to cell damage and that the muscle degeneration occurs through abnormal Ca^{2+} homeostasis caused predominantly by enhanced Ca^{2+} entry. Some drugs had significant protective effects against such mechanical weakness in vivo as well as in vitro. At present, direct targets for these drugs are not well known. However, the protective effects of Ca^{2+} handling drugs would provide valuable information for the development of novel therapeutic drugs against muscular dystrophy. Probably, more specific inhibitors against individual Ca^{2+} handling proteins would be required to be developed.

Acknowledgments

This work was supported by Grant-in-Aid for Priority Areas 13142210 and Grant-in-Aid 16590726 and 17659241 from the Ministry of Education, Culture, Sports, Science, and Technology of Japan, a grant for Promotion of Fundamental Studies in Health Science from the Organization of Pharmaceuticals and Medical Agency, research grant (16B-2) for Nervous and Mental Disorders from the Ministry of Health Labour and Welfare, grant for the Salt Science Research Foundation No. 0539 and Japan Heart Foundation Research Grant.

References

[1] Campbell KP. Three muscular dystrophies: loss of cytoskeleton-extracellular matrix linkage. Cell 1995;80:675–9.
[2] Campbell KP, Kahl SD. Association of dystrophin and an integral membrane glycoprotein. Nature 1989;338:259–62.
[3] Tinsley JM, Blake DJ, Zuellig RA, Davies KE. Increasing complexity of the dystrophin-associated protein complex. Proc Natl Acad Sci USA 1994;91:8307–13.
[4] Ervasti JM, Campbell KP. A role for the dystrophin–glycoprotein complex as a transmembrane linker between laminin and actin. J Cell Biol 1993;122:809–23.
[5] Ozawa E, Noguchi S, Mizuno Y, Hagiwara Y, Yoshida M. From dystrophinopathy to sarcoglycanopathy: evolution of a concept of muscular dystrophy. Muscle Nerve 1998;21:421–38.
[6] Crosbie RH, Lim LE, Moore SA, Hirano M, Hays AP, Maybaum SW, et al. Molecular and genetic characterization of sarcospan: insights into sarcoglycan–sarcospan interactions. Hum Mol Genet 2000;9: 2019–27.
[7] Homberger F, Baker JR, Nixon CW, Whitney R. Primary generalized polymyopathy and cardiac necrosis in an in bread line of Syrian hamsters. Med Exp 1962;6:339–48.
[8] Nigro V, Okazaki Y, Belsito A, Piluso G, Matsuda Y, Politano L, et al. Identification of the Syrian hamster cardiomyopathy gene. Hum Mol Genet 1997;6:601–7.
[9] Hack AA, Ly CT, Jiang F, Clendenin CJ, Sigrist KS, Wollmann RL, et al. Gamma-sarcoglycan deficiency leads to muscle membrane defects and apoptosis independent of dystrophin. J Cell Biol 1988;142: 1279–87.
[10] Iwata Y, Nakamura H, Mizuno Y, Yoshida M, Ozawa E, Shigekawa M. Defective association of dystrophin with sarcolemmal glycoproteins in the cardiomyopathic hamster heart. FEBS Lett 1993;329: 227–31.
[11] Duclos F, Staub V, Moore SA, Venzke DP, Hrstka RF, Crosbie RH, et al. Progressive muscular dystrophy in alpha-sarcoglycan-deficient mice. J Cell Biol 1998;142:1461–71.
[12] Brown SC, Lucy JA. Functions of dystrophin. In: Brown SC, Lucy JA, editors. Dystrophin, gene, protein and cell biology. Cambridge: Cambridge University Press; 1997. p. 163–200.
[13] Mallouk N, Jacquemond V, Allard B. Elevated subsarcolemmal Ca^{2+} in mdx mouse skeletal muscle fibers detected with Ca^{2+}-activated K^+ channels. Proc Natl Acad Sci USA 2000;97:4950–5.
[14] Robert V, Massimino ML, Tosello V, Marsault R, Cantini M, Sorrentino V, et al. Alteration in calcium handling at the subcellular level in mdx myotubes. J Biol Chem 2001;276:4647–51.
[15] Fong PY, Turner PR, Denetclaw WF, Stteinhardt RA. Increased activity of calcium leak channels in myotubes of Duchenne human and mdx mouse origin. Science 1990;250:673–6.
[16] Franco-Obregon Jr A, Lansman JB. Calcium entry through stretch-inactivated ion channels in mdx myotubes. Nature 1990;344:670–3.
[17] Sampaolesi M, Yoshida T, Iwata Y, Hanada H, Shigekawa M. Stretch-induced cell damage in sarcoglycan-deficient myotubes. Pflugers Arch 2001;442:161–70.
[18] Nakamura TY, Iwata Y, Sampaolesi M, Hanada H, Saito N, Artman M, et al. Stretch-activated cation channels in skeletal muscle myotubes from sarcoglycan-deficient hamsters. Am J Physiol 2001;281:690–9.
[19] Iwata Y, Katanosaka Y, Arai Y, Komamura K, Miyatake K, Shigekawa M. A novel mechanism of myocyte degeneration involving the Ca^{2+}-permeable growth factor-regulated channel. J Cell Biol 2003;161: 957–67.
[20] Iwata Y, Pan Y, Hanada H, Yoshida T, Shigekawa M. Dystrophin–dystrophin associated protein complex purified from hamster cardiac muscle: comparison of the complexes from cardiac and skeletal muscles of hamster and rabbit. J Mol Cell Cardiol 1996;28:2501–9.
[21] Yoshida T, Pan Y, Hanada H, Iwata Y, Shigekawa M. Bidirectional signaling between sarcoglycans and the integrin adhesion system in cultured L6 myocytes. J Biol Chem 1998;273:1583–90.
[22] Iwata Y, Shigekawa M, Wakabayashi S. Cardiac syntrophin isoforms: species-dependent expression, association with dystrophin complex and subcellular localization. Mol Cell Biochem 2005;268:59–66.
[23] Tawada-Iwata Y, Imagawa T, Yoshida A, Takahashi M, Nakamura H, Shigekawa M. Increased mechanical extraction of T-tubule/junctional SR from cardiomyopathic hamster heart. Am J Physiol 1993;264: 1447–53.
[24] Rando TA, Blau HM. Primary mouse myoblast purification, characterization, and transplantation for cell mediated gene therapy. J Cell Biol 1994;125:1275–87.
[25] Grynkiewicz G, Poenie M, Tsien RY. A new generation of calcium indicators with greatly improved fluorescence properties. J Biol Chem 1985;260:3440–50.
[26] Naruse K, Sokabe M. Involvement of stretch-activated ion channels in Ca^{2+} mobilization to mechanical stretch in endothelial cells. Am J Physiol 1993;264:C1037–44.
[27] Nie L, Oishi Y, Doi I, Shibata H, Kojima I. Inhibition of proliferation of MCF-7 breast cancer cells by a blocker of Ca^{2+}-permeable channel. Cell Calcium 1997;22:75–82.
[28] Parton RG, Way M, Zorzi N, Stang E. Caveolin-3 associates with developing T-tubules during muscle differentiation. J Cell Biol 1997; 136:137–54.
[29] McFarland DC, Singh YN, Johnson AD, Pesall JE, Gilkerson KK, vander Wal LS. Isolation and characterization of myogenic satellite cells from the muscular dystrophic hamster. Tissue Cell 2000;32: 257–65.
[30] Schneider MF, Klein MG. Sarcomeric calcium sparks activated by fiber depolarization and by cytosolic Ca^{2+} in skeletal muscle. Cell Calcium 1996;20:123–8.
[31] Menke A, Jockusch H. Decreased osmotic stability of dystrophin-less muscle cells from mdx mouse. Nature 1991;349:69–71.
[32] Franco-Obregon Jr A, Lansman JB. Mechanosensitive ion channels in skeletal muscle from normal and dystrophic mice. J Physiol (Lond) 1994;481:299–309.
[33] Alderton JM, Steinhard RA. Calcium influx through calcium leak channels is responsible for the elevated levels of calcium-dependent proteolysis in dystrophic myotubes. J Biol Chem 2000;275:9452–60.
[34] Ukai K, Masuda S, Shinoki J, Sakakura Y. Clinical and pathophysiological evaluation of tranilast in patients with pollinosis: the effects of pre-seasonal treatment. Aurisa Nasus Larynx 1993;20:275–84.
[35] Yamada H, Sugiura M, Kurihara S, Tajima S. Treatment of granuloma annulare with tranilast. J Dermatol 1995;22:354–6.
[36] Fukuyama J, Ichikawa K, Miyazawa K, Hamano S, Shiba N, Ujiie A. Tranilast suppresses intimal hyperplasia in the balloon injury model and cuff treatment model in rabbits. Jpn J Pharmacol 1996;70:321–7.
[37] Matsumura T, Kugiyama K, Sugiyama S, Ota Y, Doi H, Ogata N, et al. Suppression of atherosclerotic development in Watanabe heritable

hyperlipidemic rabbits treated with an oral antiallergic drug, tranilast. Circulation 1999;99:919–24.

[38] Ihara T, Ikeda U, Ishibashi S, Shimada K. Tranilast inhibits contraction of rat aortic smooth muscle. Eur J Pharmacol 1997;329:43–8.

[39] Yeung EW, Whitehead NP, Suchyna TM, Gottlieb PA, Sachs F, Allen D. Effects of stretch-activated channel blockers on $[Ca^{2+}]_i$ and muscle damage in the mdx mouse. J Physiol 2005;562:367–80.

[40] Hibi S, Misawa A, Tamai M, Tsunamoto K, Todo S, Sawada T, et al. Severe rhabdomyolysis associated with tacrolimus. Lancet 1995;346: 702.

[41] Liu J, Farmer Jr JD, Lane WS, Friedman LJ, Weissman I, Schreiber SL. Calcineurin is a common target of cyclosphilin-cyclosporin A and FKBP-FK506 complexes. Cell 1991;66:807–15.

[42] Norris CM, Blalock EM, Chen KC, Porter NM, Landfield PW. Calcineurin enhances L-type Ca^{2+} channel activity in hippocampal neurons: increased effect with age in culture. Neuroscience 2002;110: 213–25.

[43] Sinkins WG, Goel M, Estacion M, Schilling WP. Association of immunophilins with mammalian TRPC channels. J Biol Chem 2004;279:34521–9.

[44] Matthes J, Jager A, Handrock R, Groner F, Mehlhorn U, Schwinger RH, et al. Ca^{2+}-dependent modulation of single human cardiac L-type calcium channels by the calcineurin inhibitor cyclosporine. J Mol Cell Cardiol 2004;36:241–55.

[45] Katanosaka Y, Iwata Y, Kobayashi Y, Shibasaki F, Wakabayashi S, Shigekawa M. Calcineurin inhibits Na^+/Ca^{2+} exchange in phenylephrine-treated hypertrophic cardiomyocytes. J Biol Chem 2005;280: 5764–72.

[46] Wang T, Tsai Li, Schwartz A. Effects of verapamil, diltiazem, nisoldipine, and felodipine on sarcoplasmic reticulum. Eur J Pharmacol 1984;100:253–61.

[47] Takeo S, Elimban V, Dhalla NS. Modification of cardiac sarcolemmal Na^+–Ca^{2+} exchange by diltiazem and verapamil. Can J Cardiol 1985; 1:131–8.